# Sensitivity approach for modeling Stochastic Field of Keulegan-Carpenter and Reynolds numbers through a matrix response surface

Franck Schoefs, Morgan Boukinda

# Sensitivity Approach for Modeling Stochastic Field of Keulegan–Carpenter and Reynolds Numbers Through a Matrix Response Surface

**Franck Schoefs** **Morgan L. Boukinda**

Institute in Civil and Mechanical Engineering (GeM), Nantes Atlantic University, CNRS UMR 6183, 2 rue de la Houssinière, 44072 Nantes Cedex 03, France

*The actual challenge for requalification of existing offshore structures through a rational process of reassessment indicates the importance of employing a response surface meth-odology. At different steps in the quantitative analysis, quite a lot of approximations are performed as a surrogate for the original model in subsequent uncertainty and sensitivity studies. This paper proposes to employ a geometrical description of the nth order Stokes model in the form of a random linear combination of deterministic vectors. These vectors are obtained by rotation transformations of the wave directional vector. This facilitates introduction of an appropriate level of complexity in stochastic modeling of the wave velocity and of the Reynolds and Keulegan–Carpenter numbers for probabilistic mechan-ics analysis of offshore structures. In situ measurements are used to assess suitable ranges and distributions of basic variables.*

*Keywords: offshore structures, response surfaces, hydraulic parameters, Morison equations, wave loading*

## 1 Introduction

Nowadays one-third of the existing offshore platforms require a life extension. It is well recognized that the application of probabilistic approaches gives an efficient quantitative means for updating information and for measuring the relative change in safety level compared with a predefined requirement. During the past 2 decades, the efforts were concentrated to develop methods and corresponding software for structural reliability analyses. Increasingly in practice, failure probabilities and/or reliability indices are introduced for elaboration of load and resistance factor design (LRFD) rules [1] and comparison of design proposals. The actual challenge is to provide rational procedures and decision aid tools related to the requalification of offshore structures where the structural and mechanical integrities are important criteria.

The required structural behavior can be considered as the output of a system, which varies in response to the changing levels of several input variables. The response surface methodology (RSM) comes, of course, as a basic formal aid-tool [2,3,20]. The response curves must be based on some prescribed understanding of the underlying mechanism [4]. In particular, the time evolution of the wave propagation is usually described by second order partial differential equations within more or less simplified boundary and initial conditions, known as the Navier–Stokes equations. Useful reviews of wave loads acting on offshore structures are available in a series of articles [5,6], which focuses on the deterministic aspects mainly.

Here it is proposed to develop a formal representation of the wave kinematics field following a geometrical viewpoint. The $n$th order Stokes model has the form of a sum of $n$ vectors, each of them being obtained through suitable homothety and rotation transformations of the wave direction vector. The homothety ratios and the rotation angles are random functions for which the stochastic fluctuations depend on the wave height and on the wave kinematics intensity process. Analyzing the structure for the relevant stochastic processes leads to the derivation of a response surface for Reynolds and Keulegan–Carpenter numbers suitable for fatigue and extreme loading computation in the presence of marine growth [7].

## 2 Geometrical Modeling of the Wave Kinematics and Building of Matrix Response Surface

Physical time scales of wave actions are taken into account with practical efficiency by identifying sea-states as stationary components of a piecewise second order stationary ergodic and differentiable mean square random process [8]. As an extension of the generalized harmonic analysis, the stochastic process theory considers functions indexed by space/time parameters and with values in a so called complete probability space [9]. One way of describing a stochastic process is to specify the $n$-dimensional joint probability law whatever $n$. Another means is to give an explicit formula for the value of the process at each index point in terms of a family of random variables whose probability law is known (e.g., trajectories). The last option is retained to describe wave by wave particle velocities on jacket platforms.

There is no magic guidance to generate such formulas by selecting among mathematical models (e.g., Stokes, Boussinesq, Miche, etc.) for an application to ocean wave actions. Physical reasoning and observations give some classifications based on deterministic criteria. But these theoretical models have to be introduced in a reliability analysis, regarding their stochastic nature due to their sensitiveness to random or uncertain parameters. This drives the safety domain topology and its probability measure. To this extent a formal geometrical representation of the wave kinematics within a special care on Stokes waves is proposed.

**2.1 Matrix Response Surface of Airy Wave.** Let $(O, \boldsymbol{OX}, \boldsymbol{OY}, \boldsymbol{OZ})$ be an orthonormal basis in the Euclidean space $R^3$. The origin $O$ is taken at the mean sea level, the axis $\boldsymbol{OZ}$ is vertical and upward, and $\boldsymbol{OX}$ is the wave directional axis. The following set of time and dimensionless in space indices is considered: $t$, $x = X/l$, and $z = Z/d + 1$, where $l$ is the width of the structure (diameter of a cylinder containing the platform) and $d$ is water depth. The small amplitude plane harmonic progressive waves known as airy waves are the simplest of all solutions to the wave problem. They are derived from a velocity potential also called orthogonal stream function. The associated velocity vector $\boldsymbol{V}_{\text{Airy}}$ takes the classical form (see Eq. (1)) in the wave plane $(\boldsymbol{OX}, \boldsymbol{OZ})$

$$\boldsymbol{V}_{\text{Airy}} = \frac{H}{2}\sqrt{\frac{g}{d}\frac{\cosh(kdz)}{\cosh(kd)}}\sqrt{\frac{kd}{\tanh(kd)}}\begin{bmatrix}\cos(klx-\psi_t)\\ \tanh(kdz)\sin(klx-\psi_t)\end{bmatrix} \tag{1}$$

where $H$ is the wave height, $k$ is the wave number, $\omega$ is the (angular) frequency, and $\psi_t = \omega t - \psi$ ($\psi$ is the phase angle). The variables $k$ and $\omega$ are linked together by the one to one dispersive relation ($\omega^2 = gk\tanh(kd)$).

Equation (1) writes

$$\boldsymbol{V}_{\text{Airy}} = \lambda_1(\cos(\alpha_1)\boldsymbol{OX} + \sin(\alpha_1)\boldsymbol{OZ}) \tag{2}$$

with

$$\tan(\alpha_1) = \frac{\langle \boldsymbol{V}_{\text{Airy}}, \boldsymbol{OZ}\rangle}{\langle \boldsymbol{V}_{\text{Airy}}, \boldsymbol{OX}\rangle} = \tanh(kdz)\tan(klx - \psi_t) \tag{3}$$

$$\lambda_1 = \|\boldsymbol{V}_{\text{Airy}}\| = \frac{H}{2}\sqrt{\frac{g}{d}\frac{\cosh(kdz)}{\cosh(kd)}}\sqrt{\frac{kd}{\tanh(kd)}}\sqrt{1 - \frac{\sin^2(klx-\psi_t)}{\cosh^2(kdz)}} \tag{4}$$

The velocity vector being in the wave plane, it can be written as a combination of a homothety $\mathcal{H}$ and a rotation $\mathfrak{R}$, applied on the vector $\boldsymbol{OX}$, in the geometrical form

$$\boldsymbol{V}_{\text{Airy}} = \mathcal{H}(O, \lambda_1) o \mathfrak{R}(-\boldsymbol{OY}, \alpha_1)\boldsymbol{OX} \tag{5}$$

where $\mathcal{H}(O, \lambda_1)$ denotes the homothety with center $O$ and ratio $\lambda_1$ and $\mathfrak{R}(-\boldsymbol{OY}, \alpha_1)$ denotes the rotation of $(-\boldsymbol{OY})$ axis (with $-\boldsymbol{OV} = \boldsymbol{OX} \wedge \boldsymbol{OZ}$) and with angle $\alpha_1$.

Expression (5) allows analyzing the kinematics field (here velocity) by separating the intensity and the angle of the vector. The homothety ratio $\lambda_1$ and rotation angle $\alpha_1$ are random functions indexed by $(x, z, t)$. The fluctuations of their trajectories are depending on the couple of random variables $(H, k)$. Angle $\alpha_1$ is analytically independent of variable $H$.

The range and statistics of $k$ are well adapted to approximate the vector $\boldsymbol{W} = \mathfrak{R}(-\boldsymbol{OY}, \alpha_1)\boldsymbol{OX}$ by the normalized first order Taylor expansion $\boldsymbol{W}^{(1)}$ around the mean wave number $\overline{k}$. Subsequently some algebraic operations and differentiations are obtained as follows:

$$\boldsymbol{W}^{(1)} = \boldsymbol{W}(\overline{k}) + (k - \overline{k})\boldsymbol{W}'(k)|_{k=\overline{k}}$$

where

$$\boldsymbol{W}(\overline{k}) = \mathfrak{R}(-\boldsymbol{OY}, \underline{\alpha_1})\boldsymbol{OX} \quad \text{with} \quad \underline{\alpha_1} = \alpha_1(\overline{k}), \quad \mu_1 = (k - \overline{k})\frac{\partial \alpha}{\partial k}(\overline{k})$$

$$\begin{aligned}\boldsymbol{W}'(k)|_{k=\overline{k}} &= \underline{\alpha_1'}\mathfrak{R}\left(-\boldsymbol{OY}, \frac{\pi}{2}\right)\vec{W}(\overline{k})\\ &= \underline{\alpha_1'}\mathfrak{R}(-\boldsymbol{OY}, \underline{\alpha_1}) \circ \mathfrak{R}\left(-\boldsymbol{OY}, \frac{\pi}{2}\right)\boldsymbol{OX}\end{aligned} \tag{6}$$

Finally, $\boldsymbol{W}^{(1)}$ writes

**Table 1 Extreme sea state parameters [10]**

| |
|---|
| $H_s$: significant wave height: Gumbel distribution: $\exp(-\exp-(x-u)/\alpha)$ (e.g., 100 year period: $u = 15.5$ m; $\alpha = 1.2$) |
| $T_{\text{stat}}$: sea-state duration Exponential distribution with expectation 3 h $E(T_z \mid H_s) = \phi(H_s)$ (e.g., $\phi(H_s) = (8H_s + 21)$) |
| $H$ given $(H_s, T_{\text{stat}})$: Gumbel distribution: $\exp(-\exp-(x-u)/\alpha)$; $u = H_s\sqrt{r/2}$; $\alpha = (H_s/2)\sqrt{2r}$; $r = \log(T_{\text{stat}}/\phi(H_s))$ (e.g., 100 years: $H_s = 15.5$ m; $T_{\text{stat}} = 3$ h; $u = 28.5$; $\alpha = 1.9$) |
| $T$ given $H$: normal or lognormal distributed $E(T \mid H) = \phi(H)$ (e.g., $\phi(H_s) = \sqrt{6H + 39}$) |

$$\begin{aligned}\boldsymbol{W}^{(1)} = {} & \mathcal{H}\left(O, \frac{1}{\sqrt{1+\mu_1^2}}\right)\\ & \times o\left\{Id + \mathcal{H}(O, \mu_1) o \mathfrak{R}\left(-\boldsymbol{OY}, \frac{\pi}{2}\right)\right\} o \mathfrak{R}(-\boldsymbol{OY}, \underline{\alpha_1})\boldsymbol{OX}\end{aligned} \tag{7}$$

The goodness of the approximation can be measured through the scalar product of the two vectors (see Eq. (8)). It is given by considering in the wave plane the distance between the point $N$ of the unit circle and with coordinates $(\cos(\alpha_1 - \underline{\alpha_1}); \sin(\alpha_1 - \underline{\alpha_1}))$ and the straight line $(D)$ of equation $(X + \mu_1 Z = 0)$. Coordinates of $N$ and direction of $D$ vary with $k$. The Latin hypercube sampling technique is implemented to generate preliminary samples from the joint probability distribution for $(H, k)$ of the extreme sea-state referenced in Table 1. Figure 1 presents a simulation of this distance and statistics of $k$ around $\overline{k}$; $s$ denotes the standard deviation. It is shown that whatever the statistics, the perpendiculars to $D$ contain all the point $O$, origin of the repair and the approximation can be considered as very accurate.

$$\cos(\beta) = \langle \boldsymbol{W}^{(1)}, \boldsymbol{W}\rangle = \frac{\cos(\alpha_1 - \underline{\alpha_1}) + \mu_1\sin(\alpha_1 - \underline{\alpha_1})}{\sqrt{1+\mu_1^2}} \tag{8}$$

Introducing inside Eq. (5) the approximation $\boldsymbol{W}^{(1)}$ instead of $\boldsymbol{W}$, the velocity field corresponding has the following response curve:

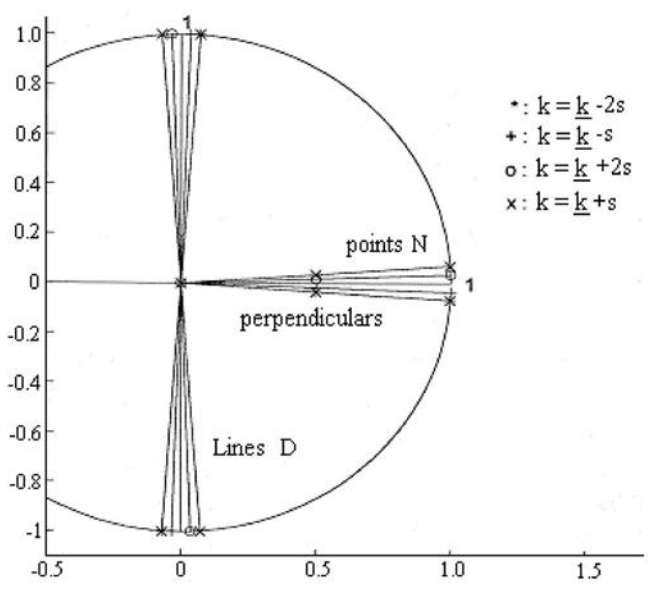


**Fig. 1 Fluctuations of *N*-(*D*) for four statistics of *k***

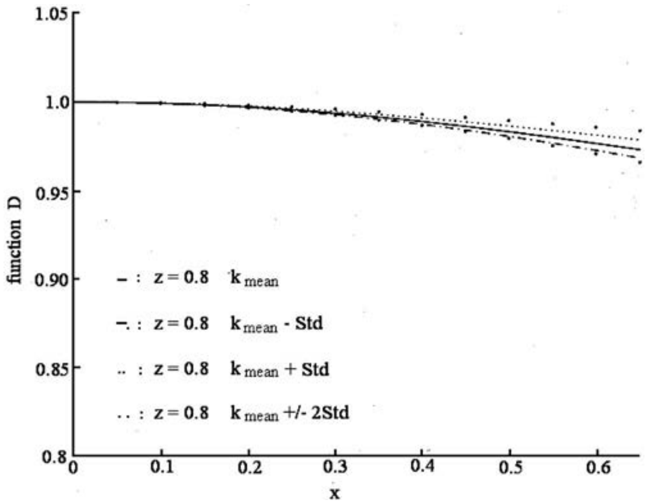


**Fig. 2 Fluctuations of $D(x,0.8,0)$ for given statistics of $k$**

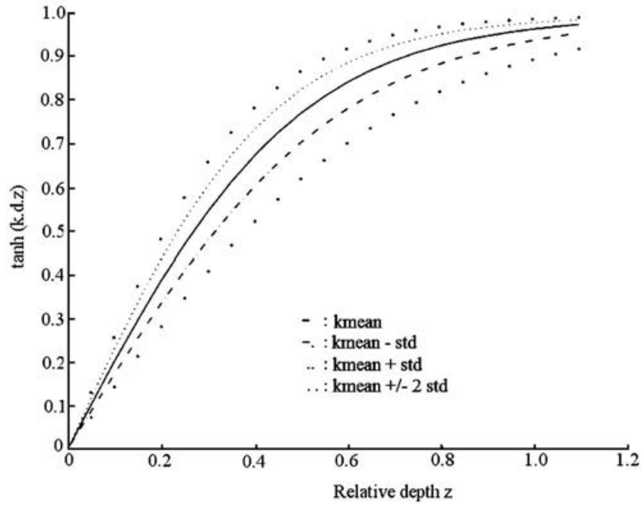


**Fig. 3 Fluctuations of $\tanh(kdz)$ $(z=0.8)$**

$$\boldsymbol{V}_{\text{Airy}} \approx \boldsymbol{V}_{\text{Airy}}^{(1)} = a_1\boldsymbol{A} + b_1\boldsymbol{B} \tag{9}$$

where $\boldsymbol{A}$ and $\boldsymbol{B}$ are deterministic orthonormal vectors defined by

$$\boldsymbol{A} = \Re(-\boldsymbol{OY}, \underline{\alpha_1})\boldsymbol{OX} \quad \text{and} \quad \boldsymbol{B} = \Re\left(-\boldsymbol{OY}, \frac{\pi}{2}\right)\boldsymbol{A}$$

and the coefficients $a_1$ and $b_1$ are random functions

$$a_1 = \frac{\lambda_1}{\sqrt{1+\mu_1^2}}, \quad b_1 = \mu_1 a_1$$

The random variable $\mu_1$ is zero-mean and with narrow support. It follows that $b_1$ is small compared with $a_1$. Consequently $\boldsymbol{A}$ represents the main axis for the velocity vector and the component following $\boldsymbol{B}$ gives the fluctuations of the velocity vector inside a narrow sector around $\boldsymbol{A}$.

**2.2 Analysis of Stochastic Structure of Airy Wave Velocity.** The previous matrix response surface format of the velocity field for airy waves allows investigation of the stochastic structure of this stochastic field through its trajectories.

*2.2.1 Role of Phase Angle $\psi$* . The pseudophase $\psi_t$ play a particular role on variability of fields defined previously. It contains a time index $t$, a hazard introduced by (angular) frequency $\omega$, and a phase which defined the position of the wave on the structure. In fact, $\psi_t$ being only in sine and cosine functions, its influence can be seen as a change in repair by translation along the wave propagation axis whose origin varies with (angular) frequency $\omega$. In the following, it is assumed that $\psi_t=0$ (e.g., initial time and the wave crest is on the first pile of the structure).

*2.2.2 Study of Stochastic Field $\lambda_1$, Wave Velocity Intensity*. The intensity of the velocity vector $\boldsymbol{V}_{\text{Airy}}$ equals $\lambda_1$. Equation (4) indicates that the scalar velocity intensity can be factorized

$$\lambda_1 = \frac{H}{2}\sqrt{\frac{g}{d}}\frac{\cosh(kdz)}{\cosh(kd)}\sqrt{\frac{kd}{\tanh(kd)}}D(k,x,z,t) \tag{10}$$

where

$$D(k,x,z,t) = \sqrt{1 - \frac{\sin^2(klx-\psi_t)}{\cosh^2(kdz)}}$$

is a function of the random variable $k$. This function varies slowly when $k$ varies on its support and is the only function indexed by $t$ and $x$. In order to illustrate this stochastic property, let us consider the extreme sea-state referenced in Table 1. Figure 2 presents the variation of $D$ versus $x$ at a depth $z=0.8$ $(Z=-20\ \text{m})$ obtained for the five statistics of $k$: mean value $\overline{k}$, mean value plus/minus standard deviation, and mean value plus/minus two times standard deviation. The coefficient of variation does not exceed 1% at this depth, which is in the wave area. Denoted by $\underline{D}$, the value of $D$ for $k=\overline{k}$, Eq. (10) is then transformed into a deterministic linear relationship (11) between two random fields

$$\lambda_1(x,z,t) = \underline{D}(x,z,0)\lambda_1^{(1)}(z) \tag{11}$$

This property is of course very interesting when investigating the stochastic properties of the wave velocity intensity. Let $M=aN$ $(a\neq 0)$ be a linear relation between two random variables. It is well known that their densities are related by $f_M(n)=1/a\ f_N(n/a)$. In particular the density $f_M$ becomes tighter when $|a|<1$.

Function $D$ is by definition upper-bounded by 1 and in the wave area, it can be shown that the term $\cosh(kdz)$ becomes dominant in comparison to $\sin(klx)$. $D$ remains in fact very close to 1 and density distributions of $\lambda_1$ will be tightening only for the highest values of $x$ in comparison to $\lambda_1^{(1)}$. Suppose now that $\psi_t\neq 0$, the assertions remain true once extended the deterministic factor to $\underline{D}(x,z,t)$ by fixing $\psi_t$ at the corresponding value to the mean wave number.

As the random velocity function $\lambda_1^{(1)}$ is indexed by $z$ only, it is deduced that the coefficient of variation and the normalized statistical moments of $\lambda_1$ (skewness, kurtosis, etc.) vary only with this profile index $z$. As a consequence, the intensity of the airy wave is a profile random function for normalized statistics.

*2.2.3 Study of the Orientation $\alpha_1$ of Velocity Vector*. When $\lambda_1$ represents the intensity of the wave velocity vector, angle $\alpha_1$ gives the main direction of this vector. It is noted that $\underline{\tanh(kdz)}$ varies slowly with $k$ and may be concentrated at its value for $k=\overline{k}$. As an illustration and for variables previously presented in Table 1, Fig. 3 plots this function varying with $x$ for the same five statistics of $k$: it is very close to $\tanh(\overline{k}dz)$ whatever $k$. For given values of $x$, the distributions of $\alpha_1$ obtained from this relationship at depth 0.8 and varying with $z$ are presented, respectively, in Figs. 4 and 5.

Then $\tan(\alpha_1)$ behaves as a deterministic linear transformation of $\tan(klx-\psi_t)$. Equation (3) can be expressed as a linear relation between two random fields

$$\tan(\alpha_1) = \beta\tan(klx-\psi_t) \quad \text{with} \quad \beta = \tanh(\overline{k}dz) \tag{12}$$

As a consequence the coefficients of variation and the normalized moments of $\alpha_1(x,z,t)$ are depending of the indices $x$ and $t$

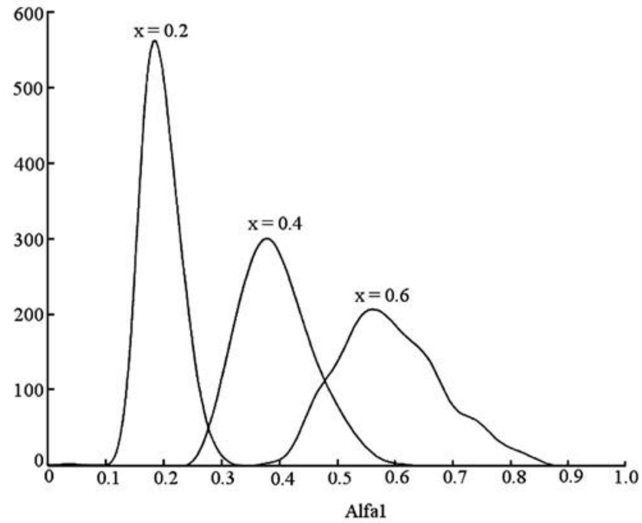


**Fig. 4 Probability density of $\alpha_1(x, 0.8)$ for three values of $x$**

only. They are constant whatever the index $z$. Moreover, in the vicinity of the mean sea level, coefficient $\beta$ is very close to 1. In this condition the angle $\alpha_1$ is well approximated as $klx - \psi_t$.

*2.2.4 Study of Stochastic Field* $\mu_1$ . From Eq. (9), the stochastic field $\mu_1$ is defined as the projection of the wave velocity vector on the deterministic vector $\boldsymbol{B}$. The stochastic analysis of $\mu_1$ is easier because this field is proportional to $(k - \overline{k})$. This stochastic field is then centered and with a similar distribution to $k$ after linear transformation. Consequently, fluctuations of $\mu_1$ are weak and its spatial variability is directly linked to the one of $\underline{\alpha_1'}$ (Eq. (13)):

$$\underline{\alpha_1'} = lx \tanh(\overline{k}dz) \frac{1 + \tan^2(\overline{k}lx)}{1 + \tan^2(\overline{k}dz)\tan^2(\overline{k}lx)} \tag{13}$$

In particular in the vicinity of the mean sea level (wave area), the approximation $\underline{\alpha_1'} = lx$ is viable. It demonstrates that $\mu_1$ is independent of the index $z$. For the study of time dependency, previous results are extended to the case $\psi_t \neq 0$,

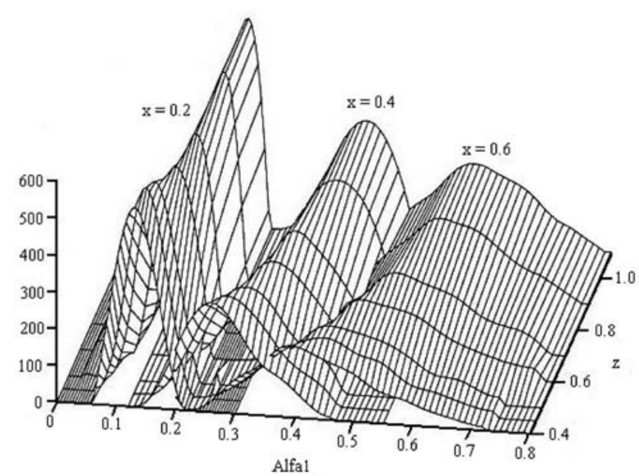


**Fig. 5 Probability density of $\alpha_1(x,z)$ for three values of $x$**

$$\underline{\alpha_1'} = \left(lx - \frac{\partial\omega}{\partial k}(\overline{k})t\right)\tanh(\overline{k}dz)\frac{1 + \tan^2(\overline{k}lx - \omega t + \varphi)}{1 + \tanh^2(\overline{k}dz)\tan^2(\overline{k}lx - \omega t + \varphi)} \tag{14}$$

In the vicinity of the mean sea level, Eq. (14) becomes

$$\underline{\alpha_1'} = \left(lx - \frac{\partial\omega}{\partial k}(\overline{k})t\right)$$

In this condition the stochastic field $\mu_1$ is linearly time dependent.

**2.3 Expansion to the Matrix Response Surface of the *n*th Order Stokes Model.** The *n*th order potential being the sum of a set of $n$ potentials, the response surface of each term $i$ is obtained by a similar transformation based on a Taylor expansion of each term (see Eq. (7)).

$$\boldsymbol{V}_i = a_i\boldsymbol{A}_i + b_i\boldsymbol{B}_i \tag{15}$$

where $\boldsymbol{A}_i$ and $\boldsymbol{B}_i$ are two deterministic orthogonal vectors in the wave plane:

$$\boldsymbol{A}_i = \Re(-\boldsymbol{OY}, \underline{\alpha_i})\boldsymbol{OX}, \quad \boldsymbol{B}_i = \Re\left(-\boldsymbol{OY}, \underline{\frac{\pi}{2}}\right)\boldsymbol{A}_i$$

$$a_i = \frac{\lambda_i}{\sqrt{1 + \mu_i^2}}, \quad b_i = \mu_i a_i$$

After projection of these vectors on $\boldsymbol{A}$ and $\boldsymbol{B}$, the response surface of *n*th order wave velocity is deduced (Eq. (16))

$$\boldsymbol{V}_n = a_n\boldsymbol{A} + b_n\boldsymbol{B} \tag{16}$$

The multipliers $a_n$ and $b_n$ are analytical random functions

$$a_n = \sum_{i=1}^{n} (a_i \cos \underline{\Delta_i} - b_i \sin \underline{\Delta_i})$$

$$b_n = \sum_{i=1}^{n} (a_i \sin \underline{\Delta_i} + b_i \cos \underline{\Delta_i}) \quad \text{where} \quad \underline{\Delta_i} = \underline{\alpha_i} - \underline{\alpha_1} \tag{17}$$

They are expressed as functions of the wave height and of the wave period. Thus their stochastic fluctuations are governed by the randomness of these basic variables. The *complexity level* is discussed when order $(n)$ is selected in the random functions $a_{(n)}$ and $b_{(n)}$. Note that each angle is deduced from relationship (18).

$$\tan(\alpha_i) = \tanh(ikdz)\tan[i(klx - \psi_t)] \tag{18}$$

By implementing previous reasoning for each order, we may conclude that in the vicinity of the mean sea level, $\alpha_i$ is well approximated to $i(klz - \psi_t)$ and thus to $i\alpha_1$. This approximation remains with depth where angles are weaker. In fact a larger relative difference may be accepted for smaller mean values. Then the approximation $\underline{\alpha_i} \approx i\underline{\alpha_1}$ may be assumed and the $\underline{\Delta_i}$ in Eq. (17) is well approximated by $(i-1)\underline{\alpha_1}$. Equation (17) makes the sensitivity analysis easier since each term of order $(n)$ can be expressed as an additional perturbation of the previous order $(n-1)$.

## 3 Matrix Response Surface of Reynolds and Keulegan–Carpenter Numbers

**3.1 General Formulation of Response Surfaces for Re and KC.** For engineering purposes, it is now well admitted that Morison equations give the main trends for the computation of hydraulic forces [11]. The set of coefficients ($C_D$, $C_M$, $C_X$, and $C_X'$) of the Morison equations depend on the hydraulic numbers: the Reynolds Re and the Keulegan–Carpenter KC numbers (Eqs. (17) and (18)) [12–15]. The American Petroleum Institute code [16] and the future ISO regulations adopt the corresponding nonlinear re-

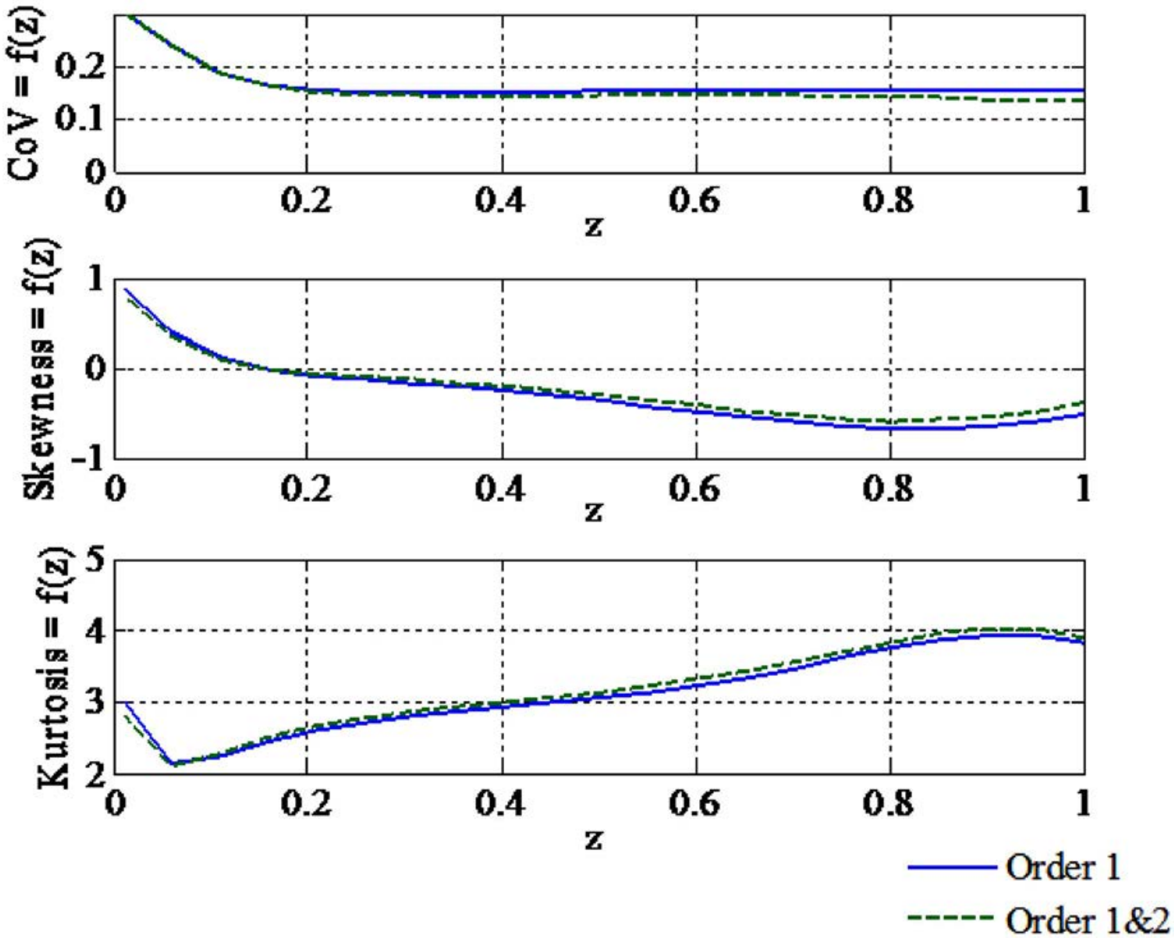


**Fig. 6 First statistics of Re as function of *z* for a vertical beam**

lationships (ISO/DIS 19902, 2004). Rather than these numbers, Stokes parameter or Strouhal number can be used.

$$\mathrm{Re} = \frac{\max_{t\in[0;T/2]}(V_{\perp}^{(n)}(t))D}{\nu} \tag{19}$$

$$\mathrm{KC} = \frac{\max_{t\in[0;T/2]}(V_{\perp}^{(n)}(t))T}{D} \tag{20}$$

where $V_{\perp}^{(n)}(t)$ is the intensity (in m/s) of the projection of the particle velocity onto the plane orthogonal to the beam, $D$ is the diameter of the beam (m), $T$ the wave period (s), and $\nu$ is the kinematics viscosity of sea water ($\mathrm{m}^2/\mathrm{s}$). Here the velocity is computed from the Stokes model of order $n$.

As a consequence, Re and KC are random fields indexed by $z$. The field of particle velocity being expressed in the plane $(O,\boldsymbol{OX},\boldsymbol{OZ})$ in global repair, local coordinates ($O_b$, $\boldsymbol{x}_b$, $\boldsymbol{y}_b$, and $\boldsymbol{z}_b$) are defined for its projection where $\boldsymbol{x}_b$ is oriented by the beam axis and $(\boldsymbol{y}_b,\boldsymbol{z}_b)$ is the plane orthogonal to the beam. By denoting $\Pi_b$, the orthogonal projection onto the beam axis and $\Pi_b\perp$ the projection onto the orthogonal plane to the beam, we obtain the response surfaces of Re and KC in Eqs. (21) and (22).

$$\mathrm{Re} = \frac{\max_{t\in[0;T/2]}\left(\left\|\prod_b \perp (a(t)_{(n)}\boldsymbol{A}(t) + b(t)_{(n)}\boldsymbol{B}(t))\right\|\right)D}{\nu} \tag{21}$$

$$\mathrm{KC} = \frac{\max_{t\in[0;T/2]}\left(\left\|\prod_b \perp (a(t)_{(n)}\boldsymbol{A}(t) + b(t)_{(n)}\boldsymbol{B}(t))\right\|\right)T}{D} \tag{22}$$

In case of vertical component and by using Eq. (16), these equations become Eqs. (23) and (24).

$$\mathrm{Re} = \frac{\max_{t\in[0;T/2]}(\|a(t)_{(n)}\cos(\underline{\alpha_1}) - b(t)_{(n)}\sin(\underline{\alpha_1})\|)D}{\nu} \tag{23}$$

$$\mathrm{KC} = \frac{\max_{t\in[0;T/2]}(\|a(t)_{(n)}\cos(\underline{\alpha_1}) - b(t)_{(n)}\sin(\underline{\alpha_1})\|)T}{D} \tag{24}$$

In case of horizontal component, they become Eqs. (25) and (26).

$$\mathrm{Re} = \frac{\max_{t\in[0;T/2]}(\|a(t)_{(n)}\sin(\underline{\alpha_1}) - b(t)_{(n)}\cos(\underline{\alpha_1})\|)D}{\nu} \tag{25}$$

$$\mathrm{KC} = \frac{\max_{t\in[0;T/2]}(\|a(t)_{(n)}\sin(\underline{\alpha_1}) - b(t)_{(n)}\cos(\underline{\alpha_1})\|)T}{D} \tag{26}$$

Note that in practice, support of distribution for $H$ and $T$ are truncated in view to represent only physical events, then maximum values can be determined.

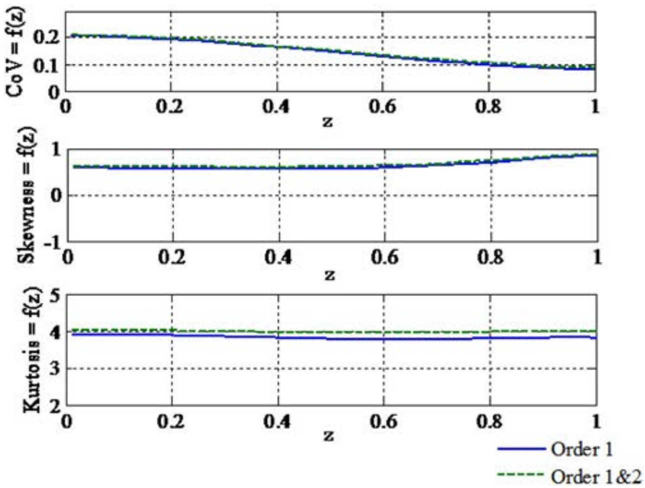


**Fig. 7 First statistics of KC as function of *z* for a vertical beam**

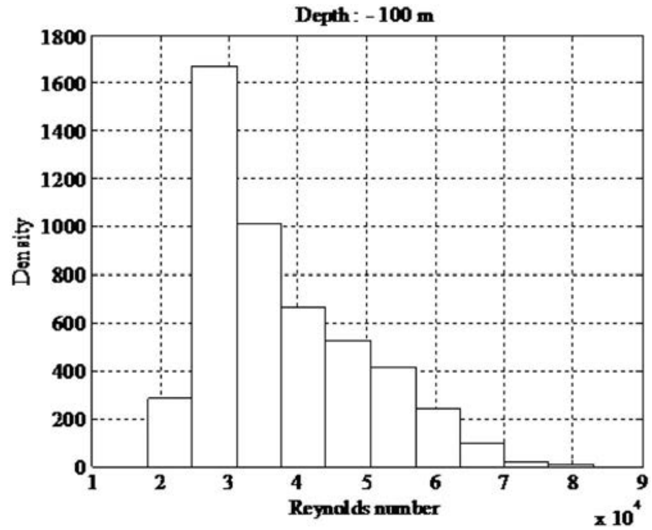


**Fig. 9 Distribution of Re for a vertical beam ($Z=-100$ m)**

**3.2 Response Surfaces in Cases of Marine Growth Presence.** In cases of marine growth presence, $D$ must be replaced in Eqs. (19)–(26) by $\theta_{mg}\ D$ where $\theta_{mg}$ is a multiplying factor. Generally, it is modeled by a random field indexed by $z$ [17].

## 4 Numerical Studies

Consider the field of extreme waves presented in Table 1. Response surfaces of Re and KC are considered. It is suggested to analyze these stochastic fields indexed by $z$ both through the evolution of statistics with depth and through the distributions at given depth. Modified Latin hypercube sampling technique is used for simulations [18]. It allows reducing the size of samples (here 1500). Convergence tests show that the relative error on variance is about 5% in this case.

Figures 6 and 7 present the evolution of the coefficient of variation, the skewness, and the kurtosis with depth for a vertical component of diameter 1 m. These statistical moments give the main information on the shape of the distribution. Only the first and the second order of the Stokes model are plotted.

First, when considering the order of the Stokes model, it is shown that the first order is sufficient to predict the main trends of the evolution with depth. It is noticed that the evolution of these statistics with depth is strong and that the coefficients of variation near the splash area ($z=1$) are, respectively, of 15% for Re and 9% for KC. Note that except at the bottom, the coefficient of variation of Re remains constant value with depth. As the mean value is strongly decreasing with depth, the variance is decreasing too. The symmetry of Re (see sign of skewness) can change with depth. This property is of significant importance for reliability studies and is underlined with Figs. 8 and 9 where distributions of Re, respectively, at depth 50 m ($z=0.5$) and 100 m ($z=0$) are given.

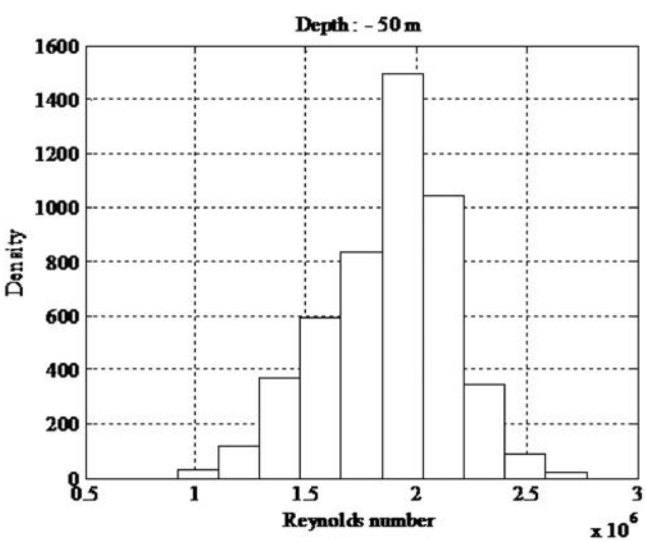


**Fig. 8 Distribution of Re for a vertical beam ($Z=-50$ m)**

## 5 Conclusions

This paper suggests a new matrix response surface for stochastic modeling of Reynolds and Keulegan–Carpenter numbers. It starts from a geometrical modeling of the wave kinematics field based on the Stokes model. The stochastic properties of the geometrical parameters are analyzed and a complete expansion is provided. It takes the form of a summation of stochastic coefficients, with known properties, with space, acting on deterministic vectors. Items such as physical meanings, complexity level in modeling, distribution effects, and computational tractability are addressed. They are essential criteria for an operational use of RSM in a reliability analysis. It allows discussing the complexity level to introduce in the Stokes model. Results are site specific and an illustration is given on a site in the North Sea [19,20]. This new approach provides an algorithmic improvement of the computer module on wave loading, which is available in different packages such as the evaluation of jackets from a probabilistic redundant analysis (ARPEJ) and the reliability analysis system for offshore structures (RASOS).

## References

[1] Joint Committee on Structural Safety, 2001, “Probabilistic Model Code,” JCSS Paper No. JCSS-OSTL/DIA/VROU-10-11-2000, www.jcss.ethz.ch.
[2] Labeyrie, J., 1990, *Stochastic Load Models for Marine Structure Reliability*, 3rd ed., IFIP WG, Berkley, CA.
[3] Schoefs, F., Le Van, A., and Rguig, M., 2008, “Cracked Finite Element for Through-Cracked Tube,” Commun. Numer. Methods Eng., **24**, pp. 761–775.
[4] Labeyrie, J., and Schoefs, F., 1995, “A Discussion on Response Surface Approximations for Use in Structural Reliability,” *Reliability and Optimization of Structural Systems*, Chapman and Hall, Assisi, Italy, pp. 161–168.
[5] Lightill, J., 1986, “Fundamentals Concerning Wave Loadings on Offshore Structures,” J. Fluid Mech., **173**, pp. 667–681.
[6] Standing, R. G., 1984, “Wave Loading on Offshore Structures, A Review,” Ocean Science and Engineering, **9**, pp. 25–134.
[7] Schoefs, F., Boukinda, M., Birades, M., Lahaille, A., and Garretta, R., 2004, “Modeling of Marine Growth Effect on Offshore Structures Loading Using Kinematics Field of Water Particle,” Proceedings of the 14th International Offshore and Polar Engineering Conference (ISOPE), Toulon, France, pp.

419–426.
[8] Labeyrie, J., 1990, “Stationary and Transient States of Random Seas,” Mar. Struct., **3**, pp. 43–58.
[9] Parzen, E., 1967, *Stochastic Process*, Holden-Day, San Francisco, CA.
[10] Doucet, Y., Labeyrie, J., and Thebault, J., 1987, “Validation of Stochastic Environmental Design Criteria in the Frigg Field,” Adv. Underwater Technol. Ocean Sci. Offshore Eng., **12**, pp. 45–59.
[11] Morison, J. R., O’Brien, M. P., Johnson, J. W., and Schaff, S. A., 1950, “The Force Exerted by Surfaces Waves on Piles,” Journal of Petroleum Technology, AIME, **189**, pp. 149–154.
[12] Sarpkaya, T., 1976, “In-line and Transverse Forces on Smooth and Sand Roughened Circular Cylinders in Oscillating Flow at High Reynolds Numbers,” Technical Report No. NPS-69SL-76062.
[13] Sarpkaya, T., 1990, “On the Effect of Roughness on Cylinders,” ASME J. Offshore Mech. Arct. Eng., **112**, pp. 334–340.
[14] Theophanatos, A., 1988, “Marine Growth and Hydrodynamic Loading of Offshore Structures,” Ph.D. thesis, University of Strathclyde, Strathclyde, UK.
[15] Wolfram, J., Jusoh, I., and Sell, D., 1993, “Uncertainty in the Estimation of the Fluid Loading Due to the Effects of Marine Growth,” ASME J. Offshore Mech. Arct. Eng., **2**, pp. 219–228.
[16] American Petroleum Institute, 2004, “Recommended Practice for Planning, Designing and Constructing Fixed Offshore Platforms—Working Stress Design,” API Report No. RP2A-WSD.
[17] Boukinda Mbadinga, M., Schoefs, F., Quiniou, V., and Birades, M., 2007, “Marine Growth Colonization Process in Guinea Gulf: Data Analysis,” ASME J. Offshore Mech. Arct. Eng., **129**(2), pp. 97–106.
[18] Iman, R. L., Helton, J. C., and Campbell, J. E., 1981, “An Approach to Sensitivity Analysis of Computer Models—Part I: Introduction, Input Variable Selection and Preliminary Variable Assessment,” J. Quality Technol., **13**(3), pp. 174–183.
[19] Schoefs, F., 1996, “Response Surface of Wave Loading for Reliability of Marine Structures,” Ph.D. thesis, University of Nantes, Nantes, France.
[20] Schoefs, F., 2008, “Sensitivity Approach for Modelling the Environmental Loading of Marine Structures Through a Matrix Response Surface,” Reliab. Eng. Syst. Saf., **93**(7), pp. 1004–1017.